



Dental development and first premolar homology in placental mammals

Festschrift in Honour of Professor Dr. Wolfgang Maier

Edited by Ingmar Werneburg & Irina Ruf

Calum J. McKay¹, Claudia Welbourn-Green², Erik R. Seiffert³, Hesham Sallam⁴, Jessica Li⁵, Sophia E. Kakarala⁶, Nigel C. Bennett⁷, Robert J. Asher⁸

¹ *Alumnus of Emmanuel College and the Department of Zoology, University of Cambridge, United Kingdom*

² *Alumna of Pembroke College, University of Cambridge, United Kingdom*

³ *Department of Integrative Anatomical Sciences, Keck School of Medicine, University of Southern California, Los Angeles, California, USA*

⁴ *Institute of Global Health and Human Ecology, American University in Cairo, New Cairo and Mansoura University Vertebrate Paleontology Center, Department of Geology, Mansoura University, Egypt*

⁵ *Alumna of Robinson College, University of Cambridge, United Kingdom*

⁶ *Alumna of Clare College Cambridge and Weill Cornell Medicine, New York, USA*

⁷ *Mammal Research Institute, Department of Zoology and Entomology, University of Pretoria, South Africa*

⁸ *Department of Zoology and Trinity Hall, University of Cambridge, United Kingdom*

<http://zoobank.org/7F6DD9E1-AA95-4DF9-B3E1-03B9871B3AD6>

Corresponding author: Robert J. Asher (r.asher-at-zoo.cam.ac.uk)

Academic editor Ingmar Werneburg | **Received** 24 November 2021 | **Accepted** 4 April 2022 | **Published** 20 May 2022

Citation: McKay CJ, Welbourn-Green C, Seiffert ER, Sallam H, Li J, Kakarala SE, Bennett NC, Asher RJ (2022) Dental Development and First Premolar Homology in Placental Mammals. *Vertebrate Zoology* 72 201–218. <https://doi.org/10.3897/vz.72.e78234>

Abstract

Macroscelidid afrotherians and canid carnivorans possess four premolar loci, the first of which is not replaced. Previous work suggests that the first premolar in macroscelidids is a retained deciduous tooth, but in *Canis* it is a successional tooth with no milk precursor. We tested this contrasting interpretation of first premolar homology with data from ontogenetic anatomy and with area predictions from the inhibitory cascade (IC) model. Our results based on anatomy support previous interpretations that the functional first premolar is a retained deciduous tooth (dp1) with no successor in macroscelidids, and a successional tooth (p1) with no precursor in *Canis*. Hyracoids are among the few placental mammals that show replacement at the first premolar locus and show less deviation than other taxa of actual from predicted areas across the deciduous and molar tooththrow. However, predicted vs. actual tooth areas can depart substantially from one another. At least without a better means of representing tooth size, the inhibitory cascade does not help to distinguish the deciduous from successional first premolar. This observation does not rule out the possibility that factors such as a size-shift within the tooththrow (e.g., carnivoran carnassials) help to explain deviations from the inhibitory cascade model.

Keywords

Afrotheria, canids, Carnivora, deciduous teeth, dogs, macroscelidids, ontogeny, tooth replacement, sengis

Introduction

Living mammals show remarkably consistent patterns of growth and morphology in their dentitions. Most have four readily identifiable dental types: incisors, canines, premolars (collectively known as antemolars) and molars (Maier 1984). Groups such as rodents and lagomorphs lack canines and anterior premolars. Monotremes, xenarthrans, aardvarks, pangolins, cetaceans and aquatic carnivorans further lose some or all tooth types. With very few exceptions (Domning and Hayek 1984; Gomes-Rodrigues et al. 2011), and documented by an extensive fossil record (O'Meara and Asher 2016), mammalian teeth are replaced just once, if at all. In marsupials, antemolar replacement is limited to the last premolar; other species lack premolar replacement altogether (Van Nievelt and Smith 2005), either because the deciduous (e.g., soricids) or replacement (e.g., proboscideans) generation never fully mineralizes or breaks the gum. Tooth types and deciduous vs. permanent generations are usually distinguishable in most species based on their anatomy and eruption patterns (Ungar 2010).

When postnatal anatomy is not sufficient to recognize positional or ontogenetic dental homologies, embryonic development has played a key role (Luckett and Maier 1982; Luckett 1993a, b; Van Nievelt and Smith 2005). Nineteenth and early 20th century studies of dental ontogeny extensively utilized juvenile and embryonic specimens (e.g., Tomes 1874, 1897; Leche 1907; Butler 1937), and indeed our understanding of dental development arises from such material. As summarized by Williams and Evans (1978), Luckett (1993a), Järvinen et al. (2009), and others, mammalian teeth of both the deciduous and permanent dentitions undergo the same ontogenetic stages during development: bud, cap, and bell, each subdivided into early, middle and late. The primary dental lamina in mammals has a restricted capacity to generate successional teeth, and its regression limits the dentition to two generations (Popa et al. 2016). The deciduous dentition and molars have long been regarded as arising from the embryonic primary dental lamina, connected to the oral epithelium (Owen 1845; Butler 1937). While molars are functionally part of the permanent dentition, their apparent origin from the primary dental lamina would make them, developmentally speaking, late-erupting “deciduous” teeth (Luckett 1993a; Tucker and Fraser, 2014). Replacement teeth arise from the lingual successional lamina of their corresponding deciduous precursors (Butler 1937), although origins from a primary or successional lamina is not always obvious in cases when one or the other is vestigial (see Van Nievelt and Smith 2005, discussed further below).

The first premolar locus has regressed in nearly all placental mammals to just one generation or none at all. First premolar replacement has been documented in some fossil groups, including hyracoids (Gheerbrant et al. 2007; Asher et al. 2017) and cetaceans (Uhen 2000). Among living groups, first premolar replacement consistently occurs only in the upper dentition of *Tapirus* (Ziegler 1971),

but may also occur in some individuals of *Procapra* (Asher et al. 2017). The xenarthran genus *Dasyurus* typically exhibits seven or eight replaced, antemolar teeth in each quadrant, without obvious homologies of any of them to the antemolars of other mammals (Ciancio et al. 2012). A single generation at the first premolar characterizes many carnivorans, artiodactyls, perissodactyls, talpids, and macroscelidids. Otherwise, the first premolar locus is absent in living mammals.

Kindahl (1957, 1967) argued that the macroscelidid first premolar was a retained deciduous tooth. She collected data from five histologically prepared embryos of *Elephantulus myurus* of 16mm, 17mm, 19mm, 25mm, and 40mm greatest length, as well as osteological specimens. She observed in her embryos that the anterior-most premolar arose from the primary dental lamina, and never observed a successional lamina (or in later stages a replacement tooth) arising from that locus. Kindahl (1957:29) therefore concluded that “the first premolar [of *Elephantulus*] belongs to the lacteal set of teeth”, or dp1.

Williams and Evans (1978) suggested the opposite for domesticated dogs (beagles) based on 172 specimens of known age. Of these, 29 were histologically sectioned and 143 were cleared and stained; sizes ranged from 12–95mm CRL (histology) and 20–166mm (cleared and stained), representing developmental ages of approximately 25–63 days post coitus, corresponding roughly to the last 5.4 weeks of a 9 week pregnancy. In their sample, the primary dental lamina between tooth buds of the dp2 and canine remained undeveloped throughout most of prenatal ontogeny. Only at later stages, from 42–47 days, did signs of bud initiation corresponding to the first premolar locus appear, temporally coincident with the initiation of the permanent replacements of deciduous teeth. Williams and Evans (1978: 161) tentatively concluded that “the first premolars develop in the late fetus and are regarded here as teeth of the permanent dentition without deciduous predecessors”.

The positive evidence used by both Williams and Evans (1978) and Kindahl (1957) concerned the morphology of the primary dental lamina and timing of mineralization. On the other hand, neither Kindahl (1957) nor Williams and Evans (1978) observed specimens in possession of a rudimentary, partly formed dp1 or p1 simultaneously with its cognate. In principle, one or few observations of a developing successional tooth connected to a dp1 could alter their conclusions on the homology of the tooth at the first premolar locus.

Here, we build on the work of past authors to examine homology of the first premolar locus and test the hypothesis that the functional, first premolar locus in each belongs to separate generations: the dp1 in macroscelidids and the p1 in canids. We focus primarily on these two groups given the contrasting interpretations of their first premolar homologies, and for comparison examine other carnivorans and afrotherians, in particular hyracoids, as they are among the only mammals with documented replacement at the first premolar locus (Gheerbrant et al. 2007; Asher et al. 2017). We use microCT scans and histologically-prepared specimens to try and identify re-

placement at the p1 locus in growth stages that previous authors may have missed.

We furthermore consider the inhibitory cascade hypothesis (IC, Kavanagh et al. 2007; Polly 2007; Wilson et al. 2012; Evans et al. 2016) to determine if its predictions of size can distinguish between deciduous and replacement teeth at the first-premolar locus. There are many instances in which inhibitory cascade predictions depart from observed molar areas (Renvoisé et al. 2009; Asahara 2013; Evans et al. 2016; Roseman and Delezene 2019). Its applicability to deciduous premolar sizes is less well known. If it does predict areas of known deciduous premolars, then it may be useful to distinguish deciduous vs. replacement teeth at loci in which replacement has not yet been observed, such as the first premolar.

Methods

We employed two methods to test the developmental homology of teeth at the p1 locus. First, we assembled a dataset of skeletal (Table 1) and soft-tissue stained (Table 2) CT scanned prenatal and juvenile specimens that could in theory show evidence for replacement at this locus, to which we added four histologically prepared macroscelidids, one canid, and made comparisons to six hyracoids (Table 3). Second, we measured linear dimensions of deciduous and permanent generations from the lower canine to last molar to determine if tooth area can be predicted based on the inhibitory cascade model (Kavanagh et al. 2007; Evans et al. 2016). This was articulated by Evans et al. (2016) as $B=0.5(A+C)$, algebraically equivalent to $A=2B-C$ and $C=2B-A$, where A, B, and C represent two-dimensional areas of each of three adjacent teeth (in their case, molars) derived from the primary dental lamina. If tooth area follows the inhibitory cascade, then the middle tooth of a triplet would have an area approximating the average of the areas of the first and third ($B=0.5(A+C)$); the first tooth would have an area about twice the second minus the third ($A=2B-C$); the last tooth would have an area about twice the second minus the first ($C=2B-A$). Therefore, following Kindahl's (1957) interpretation, the first premolar of *Elephantulus* (dp1) should have an area approximating twice that of dp2 minus dp3. We would similarly expect a dp1 of *Canis* to correspond more than a p1 to an area approximating twice that of dp2 minus dp3.

In order to be consistently measurable, tooth crowns have to be at or close to full mineralization. It would also be ideal to have measurements across all loci to be able to test area predictions for any tooth arising from the primary dental lamina. In reality, a full complement of molars rarely co-occurs with all deciduous teeth, and area estimates for conical, trenchant teeth are more prone to error than those from rectangular, molariform teeth. Therefore, we did not test predictions for loci anterior to the first premolar. Of the three equations noted above to predict tooth area using the inhibitory cascade, we used whichever

applied to one individual's available teeth without assuming first premolar homology. For example, to predict size of an m1, we used $C=2B-A$ ($2 \times dp4 - dp3$) unless dp3 or dp4 were missing, in which case we used $B=(A+C)/2$ ($(dp4+m2)/2$) unless dp4 or m2 were missing, in which case we used $A=2B-C$ ($2 \times m2 - m3$). For predicting dp2 area we used only $A=2B-C$ and for dp3, either $A=2B-C$ or $B=(A+C)/2$ in order to avoid using the first premolar to predict areas of other loci. In addition, because incisors lack clear landmarks with which to define length and width, we omitted incisors from our sample, using instead teeth between (and including) the canine and the last molar. We made length and width measurements based on 3D rendered CT scans (and did not try to measure teeth from histological specimens) using Drishti (versions 2.6.4 to 2.7, Limaye 2012) as per the landmarks shown in Figure 1.

We sampled postnatal and soft-tissue stained embryonic specimens across 13 species in 9 genera of afrotherians and carnivorans. Our sample of CT-scanned *Canis* specimens consists of multiple species and subspecies, including two coyotes (*C. latrans*), two Mexican wolves (*C. lupus baileyi*), two arctic wolves (*C. lupus arctos*), a wolf (*C. lupus*) native to Lebanon, and seven domestic dogs (*C. lupus familiaris*). Six of the latter are pointers, five of which have known ages. Age post-birth was also known for 16 specimens of *Macroscelides* (Table 1 and Asher and Olbricht 2009). While the anterior-most premolariform cheektooth in *Procavia* has sometimes been interpreted as a canine (Lockett 1993b), based on data from Asher et al. (2017) and Gomes-Rodrigues et al. (2019) we regard it as a first premolar. All of the other genera are uncontroversially known to typically possess four permanent premolars. Most also have three molars, except for *Otocyon* (with four) and *Macroscelides*, *Nandinia*, *Nasua* and *Viverra* (with two). For soft-tissue stained CT scans (Table 2), we followed the PTA (phosphotungstic acid) protocol described by Metscher (2009: table 2). Supplementary appendix S1 provides measurements and details on individual specimens in csv format.

Our sample is limited by the number of specimens that simultaneously possess a measurable first premolar along with adjacent deciduous teeth that allow for calculation of dp1 area according to the inhibitory cascade. This has the advantage of not averaging across specimens that may vary in size due to unrelated factors (e.g., variation among breeds), but on the other hand reduces our sample size. For example, *Canis* is a common species, well-represented in museum collections and the literature, but even when developmental series are available, they rarely exhibit specimens with a fully mineralized first premolar crown along with measurable dp2 and dp3. Hence, we have just one *Canis* specimen in our sample providing both predicted and observed areas for the first premolar, as detailed below.

Throughout the text, we use dental abbreviations that correspond with our results and those of Kindahl (1957) and Williams and Evans (1978). That is, we describe macroscelidids with a retained dp1/dP1 and *Canis* with an unreplaced p1/P1. Individual teeth are abbreviated

Table 1. Non-stained specimens examined using microCT. Institutional abbreviations are **BMNH (also NHM, NHMUK)** = Natural History Museum London UK, **CBC** = Cambridge Biotomography Centre UK, **DPC** = Duke Primate Center USA, **DU-EA** = Duke University Department of Evolutionary Anthropology, **FMNH** = Field Museum of Natural History Chicago USA, **ISEM** = Institute of Evolutionary Science of Montpellier France, **MNHN** = Muséum National d'Histoire Naturelle Paris France, **MS** = www.morphosource.org USA, **NHM (and BMNH, NHMUK)** = Natural History Museum London UK, **UCL** = University College London, **UMZC** = University Museum of Zoology Cambridge UK, **USNM** = United States National Museum Washington USA, **YPM** = Yale Peabody Museum New Haven USA. Sizes are given in millimeters.

genus	species	collection	accession (field #)	voxel XY	voxel Z	age in days	source
<i>Macroselides</i>	<i>proboscideus</i>	UMZC	2011.1.8 (w60)	0.0259713	0.0259713	0	UCL-skyscanner
<i>Macroselides</i>	<i>proboscideus</i>	UMZC	2011.1.3 (w50)	0.02091	0.02091	2	UCL-skyscanner
<i>Macroselides</i>	<i>proboscideus</i>	UMZC	2011.1.6 (w57)	0.0098815	0.0098815	3	CBC
<i>Macroselides</i>	<i>proboscideus</i>	UMZC	2011.1.7 (w58)	0.0112248	0.0112248	3	CBC
<i>Macroselides</i>	<i>proboscideus</i>	UMZC	2011.1.4 (w53)	0.0131805	0.0131805	16	CBC
<i>Macroselides</i>	<i>proboscideus</i>	UMZC	2022.2.1 (w43)	0.0179002	0.0179002	38	CBC
<i>Macroselides</i>	<i>proboscideus</i>	UMZC	2021.37 (w3)	0.0163798	0.0163798	69	CBC
<i>Macroselides</i>	<i>proboscideus</i>	UMZC	2022.2.2 (w11)	0.0171758	0.0171758	101	CBC
<i>Macroselides</i>	<i>proboscideus</i>	UMZC	2022.2.3 (w64)	0.0178620	0.0178620	113	CBC
<i>Macroselides</i>	<i>proboscideus</i>	UMZC	2022.2.4 (w15)	0.0171758	0.0171758	122	CBC
<i>Macroselides</i>	<i>proboscideus</i>	UMZC	2022.2.5 (w37)	0.13	0.13	145	Cam-Engineering
<i>Macroselides</i>	<i>proboscideus</i>	UMZC	2022.2.6 (w30)	0.0172439	0.0172439	157*	CBC
<i>Macroselides</i>	<i>proboscideus</i>	UMZC	2022.2.7 (w45)	0.0172743	0.0172743	195	CBC
<i>Macroselides</i>	<i>proboscideus</i>	UMZC	2021.38 (w39)	0.0174388	0.0174388	326*	CBC
<i>Macroselides</i>	<i>proboscideus</i>	UMZC	2022.2.8 (w12)	0.0176474	0.0176474	426	CBC
<i>Macroselides</i>	<i>proboscideus</i>	UMZC	2022.2.9 (w56)	0.0178080	0.0178080	1982	CBC
<i>Macroselides</i>	<i>proboscideus</i>	FMNH	137045	0.0386790	0.0773580		MS
<i>Procavia</i>	<i>capensis</i>	UMZC	H4981E	0.0391484	0.0391484		CBC
<i>Procavia</i>	<i>capensis</i>	UMZC	H4980K	0.0427502	0.0427502		CBC
<i>Procavia</i>	<i>capensis</i>	UMZC	H4981C	0.0371703	0.0371703		CBC
<i>Procavia</i>	<i>capensis</i>	UMZC	H4981D	0.0357073	0.0357073		CBC
<i>Procavia</i>	<i>capensis</i>	UMZC	H5051A	0.0439436	0.0439436		CBC
<i>Procavia</i>	<i>capensis</i>	UMZC	H4980J	0.0448615	0.0448615		CBC
<i>Procavia</i>	<i>capensis</i>	UMZC	H5101A	0.0465609	0.0465609		CBC
<i>Procavia</i>	<i>capensis</i>	MNHN	1901_685f	0.0358120	0.0358120		ISEM
<i>Procavia</i>	<i>capensis</i>	UMZC	H5081A	0.0576404	0.0576404		CBC
<i>Procavia</i>	<i>capensis</i>	UMZC	H5081B	0.0537667	0.0537667		CBC
<i>Canis</i>	<i>latrans</i>	UMZC	K3341	0.1250480	0.1250480		MS
<i>Canis</i>	<i>latrans</i>	UMZC	K3348	0.0548351	0.0548351		CBC
<i>Canis</i>	<i>lupus familiaris</i>	UMZC	K3051	0.0788500	0.0788500		CBC
<i>Canis</i>	<i>lupus familiaris</i>	UMZC	K3014	0.0634513	0.0634513		CBC
<i>Canis</i>	<i>lupus</i>	UMZC	K3150.3	0.1250790	0.1250790		CBC
<i>Canis</i>	<i>lupus arctos</i>	USNM	291012	0.270	0.250		MS
<i>Canis</i>	<i>lupus arctos</i>	USNM	507338	0.270	0.250		MS
<i>Canis</i>	<i>lupus baileyi</i>	USNM	98311	0.242	0.250		MS
<i>Canis</i>	<i>lupus baileyi</i>	USNM	98037	0.243	0.250		MS
<i>Canis</i>	<i>lupus familiaris</i>	BMNH	1919-7-7-3633	0.019997	0.019997	1	NHM
<i>Canis</i>	<i>lupus familiaris</i>	BMNH	1919-7-7-3634	0.022596	0.022596	5	NHM
<i>Canis</i>	<i>lupus familiaris</i>	BMNH	1919-7-7-3635	0.028572	0.028572	10	NHM
<i>Canis</i>	<i>lupus familiaris</i>	BMNH	1919-7-7-3636	0.029990	0.029990	18	NHM
<i>Canis</i>	<i>lupus familiaris</i>	BMNH	1919-7-7-3644	0.039289	0.039289	33	NHM
<i>Canis</i>	<i>lupus familiaris</i>	BMNH	2005-205	0.028761	0.028761		NHM
<i>Nandinia</i>	<i>binotata</i>	USNM	450440	0.0483000	0.1057000		MS
<i>Nandinia</i>	<i>binotata</i>	USNM	220397	0.0518000	0.1158000		MS
<i>Nandinia</i>	<i>binotata</i>	YPM	14716	0.0774565	0.0774565		MS
<i>Nandinia</i>	<i>binotata</i>	UMZC	K4492	0.1007061	0.1007061		CBC
<i>Nandinia</i>	<i>binotata</i>	UMZC	K4494	0.0517450	0.0517450		CBC
<i>Nandinia</i>	<i>binotata</i>	UMZC	K4493	0.0549597	0.0549597		CBC
<i>Nandinia</i>	<i>binotata</i>	UMZC	K4490	0.0565852	0.0565852		CBC
<i>Nandinia</i>	<i>binotata</i>	BMNH	26.7.6.162	0.0288620	0.0288620		NHM

genus	species	collection	accession (field #)	voxel XY	voxel Z	age in days	source
<i>Nandinia</i>	<i>binotata</i>	BMNH	46.356	0.0320520	0.0320520		NHM
<i>Nasua</i>	sp.	DU-EA	182	0.0491022	0.0491022		MS
<i>Nasua</i>	<i>narica</i>	UMZC	K1586	0.0765217	0.0765217		CBC
<i>Nasua</i>	<i>narica</i>	UMZC	K1588	0.0661318	0.0661318		CBC
<i>Nasua</i>	<i>narica</i>	UMZC	K1589	0.0726409	0.0726409		CBC
<i>Nasua</i>	<i>nasua</i>	UMZC	K1594	0.0675932	0.0675932		CBC
<i>Nasua</i>	<i>nasua</i>	BMNH	75.2334	0.0345260	0.0345260		NHM
<i>Nasua</i>	<i>nasua</i>	BMNH	3.7.1.21	0.0389540	0.0389540		NHM
<i>Otocyon</i>	<i>megalotis</i>	USNM	429129	0.0703	0.1529		MS
<i>Otocyon</i>	<i>megalotis</i>	USNM	429132	0.0703	0.1529		MS
<i>Otocyon</i>	<i>megalotis</i>	UMZC	K3942	0.0624674	0.0624674		CBC
<i>Otocyon</i>	<i>megalotis</i>	BMNH	26.12.7.68	0.0288620	0.0288620		NHM
<i>Otocyon</i>	<i>megalotis</i>	BMNH	26.12.7.69	0.0288620	0.0288620		NHM
<i>Viverra</i>	<i>zibetha</i>	FMNH	104395	0.1074430	0.2148860		MS
<i>Viverra</i>	<i>zibetha</i>	UMZC	K4262	0.0809521	0.0809521		CBC
<i>Viverra</i>	sp.	UMZC	K4258	0.0530884	0.0530884		CBC
<i>Viverra</i>	<i>zibetha</i>	UMZC	K4264	0.0384579	0.0384579		CBC
<i>Viverra</i>	sp.	UMZC	K4265	0.0625242	0.0625242		CBC
<i>Viverra</i>	<i>tangalanga</i>	BMNH	99.12.9.16	0.0320520	0.0320520		NHM
<i>Sagatherium</i>	<i>bowni</i>	DPC	17844	0.0478470	0.0478470		DPC
<i>Sagatherium</i>	<i>bowni</i>	DPC	24040	0.0345811	0.0345811		DPC
<i>Sagatherium</i>	<i>bowni</i>	DPC	11684	0.0478470	0.0478470		DPC
<i>Sagatherium</i>	<i>bowni</i>	DPC	16527	0.0310250	0.0310250		DPC
<i>Sagatherium</i>	<i>bowni</i>	DPC	13282	0.0478367	0.0478367		DPC
<i>Sagatherium</i>	<i>bowni</i>	DPC	12048	0.0644028	0.0644028		DPC
<i>Sagatherium</i>	<i>bowni</i>	DPC	11451	0.0443151	0.0443151		DPC
<i>Sagatherium</i>	<i>bowni</i>	DPC	16845	0.0478367	0.0478367		DPC
<i>Sagatherium</i>	<i>bowni</i>	DPC	11919	0.0457014	0.0457014		DPC
<i>Thyrohyrax</i>	<i>litholagus</i>	DPC	18227	0.0526196	0.0526196		DPC
<i>Thyrohyrax</i>	<i>litholagus</i>	DPC	20624	0.0526196	0.0526196		DPC
<i>Thyrohyrax</i>	<i>litholagus</i>	DPC	21027	0.0418587	0.0418587		DPC
<i>Thyrohyrax</i>	<i>meyeri</i>	DPC	9591	0.0417210	0.0417210		DPC
<i>Thyrohyrax</i>	<i>meyeri</i>	DPC	20828	0.0478367	0.0478367		DPC
<i>Thyrohyrax</i>	<i>meyeri</i>	DPC	17675	0.0644028	0.0644028		DPC
<i>Thyrohyrax</i>	<i>meyeri</i>	DPC	20777	0.0478470	0.0478470		DPC
<i>Thyrohyrax</i>	<i>meyeri</i>	DPC	17017	0.0478470	0.0478470		DPC
<i>Thyrohyrax</i>	<i>meyeri</i>	DPC	17603†	0.0280945	0.0280945		DPC
<i>Thyrohyrax</i>	<i>meyeri</i>	DPC	23864†	0.0243776	0.0243776		DPC

* Asher and Olbricht 2009: table 1 mistakenly reported 150 days for UMZC 2022.2.6 (w30) and 330 days for UMZC 2021.38 (w39); values shown here are correct.

† Asher et al. (2017) misidentified the dentitions of two jaw fragments of *T. meyeri*, DPC 17603 and DPC 23864. The former consists of a right i3, canine followed by p1-4 (not c, p1-m1) and the latter of a right canine followed by p1-p4 (not p1-m1).

Table 2. PTA stained specimens (Phosphotungstic Acid, see Metscher 2009: table 2) examined with microCT. HL = Head Length, CRL = Crown Rump Length. Sizes (voxel, HL, CRL) are given in millimeters.

genus	species	collection	accession (field #)	voxel XY	voxel Z	source	HL	CRL
<i>Elephantulus</i>	<i>myurus</i>	UMZC	2022.1.1 (GES 10.2)	0.0054148	0.0054148	CBC	5.5	9.5
<i>Elephantulus</i>	<i>myurus</i>	UMZC	2022.1.2 (Pretoria 9.9)	0.0071535	0.0071535	CBC	10	13.4
<i>Elephantulus</i>	<i>myurus</i>	NRM	Em30	0.0073737	0.0073737	CBC	11	14.2
<i>Elephantulus</i>	<i>myurus</i>	UMZC	2022.1.3 (GES 10.4B)	0.0086893	0.0094590	CBC		15
<i>Elephantulus</i>	<i>myurus</i>	UMZC	2022.1.4 (GES 10.3)	0.0095864	0.0095864	CBC	14.7	18.1
<i>Elephantulus</i>	<i>myurus</i>	UMZC	2022.1.5 (Pretoria 5.5)	0.0111855	0.0111855	CBC	17.25	21.4

with “i” for incisor, “c” for canine, “p” for premolar, “m” for molar, the prefix “d” to indicate deciduous antemolars, and (unless specified otherwise) upper and lower-

case for upper and lower teeth (respectively). Numbers follow serial homologies as used by Butler (1937) and illustrated by Asher (2019).

Table 3. Histology specimens. CRL = crown rump length, HE = Hematoxylin and Eosin stain, HL = head length, NRM = National Riksmuseet Stockholm, um = micron or 0.001 mm, UMZC = University Museum of Zoology Cambridge

genus	species	collection	accession	slice thickness (um)	HL	CRL	stain
<i>Canis</i>	<i>lupus familiaris</i>	UMZC	2016-histo-Cd1	10		60	HE
<i>Elephantulus</i>	<i>myurus</i>	UMZC	2016-histo-Ep1	10	11.5		Masson
<i>Elephantulus</i>	<i>myurus</i>	UMZC	2016-histo-Ep2	10	16.5		Masson
<i>Elephantulus</i>	<i>myurus</i>	UMZC	2019-histo-EL1	10		47	alternating HE-Trichrome
<i>Petrodromus</i>	<i>tetradactylus</i>	UMZC	2016-histo-Pd5	10	15	31	Masson
<i>Procavia</i>	<i>capensis</i>	NRM	14G1	10		28	trichrome
<i>Procavia</i>	<i>capensis</i>	NRM	18G1	10		26	trichrome
<i>Procavia</i>	<i>capensis</i>	NRM	19G1	10		29	trichrome
<i>Procavia</i>	<i>capensis</i>	NRM	38G1	20		42	trichrome
<i>Procavia</i>	<i>capensis</i>	NRM	39G1	30		60	alternating HE-Trichrome
<i>Procavia</i>	<i>capensis</i>	NRM	40G1	40		80	trichrome

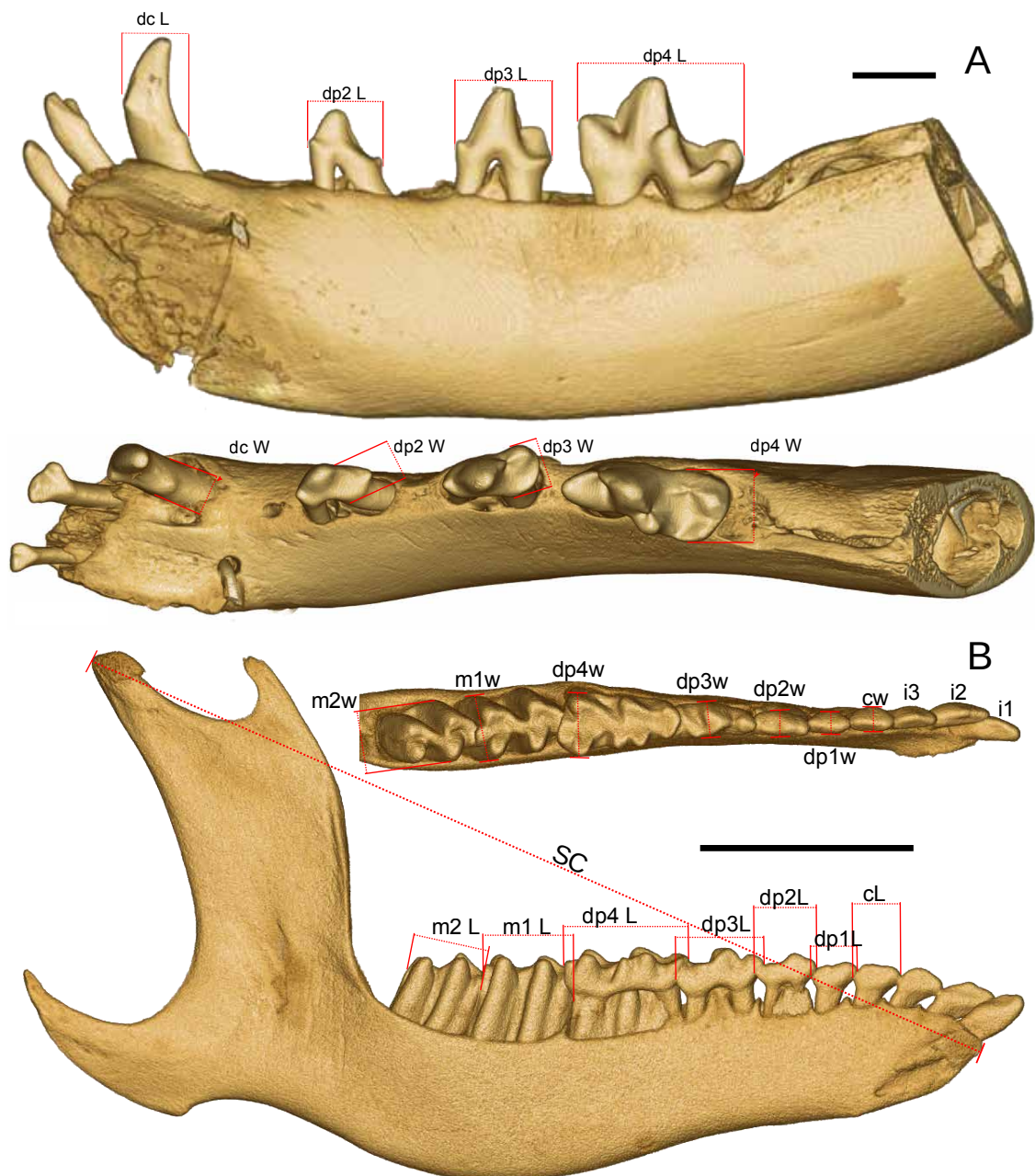


Figure 1. Guide to linear measurements of length and width shown in red. **A**) shows lingual (top) and occlusal (bottom) views of *Canis familiaris* (UMZC K3051). **B**) shows occlusal (top) and lingual (bottom) views of *Macroscelides proboscideus* (UMZC 2022.2.2). “L” and “W” indicate length and width, respectively; “SC” = symphysis to condyle distance; scale bars = 5mm.

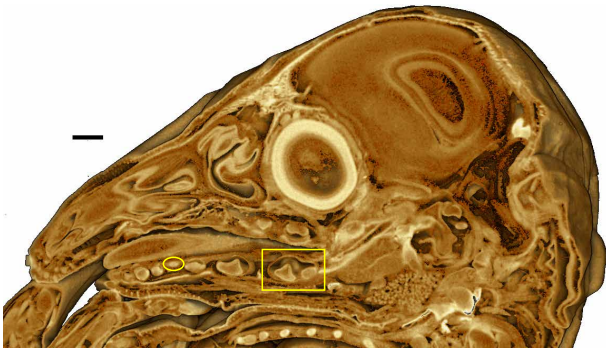


Figure 2. Soft-tissue stained CT reconstruction of an embryonic *Elephantulus myurus* (UMZC 2022.1.5, CRL 21.4, HL 17.25mm) showing sagittal section through head with exposed left lower and partial upper dentition. Square indicates dp4 and circle dp1. Scale bar = 1mm

Results

Comparative developmental anatomy: macroscelidids and *Procavia*

Histologically prepared specimens of *Elephantulus myurus* show eight tooth buds originating from the primary dental lamina in both the upper and lower dentitions, comprising upper and lower di1–3, dc, and dp1–4. Our specimen of *Petrodromus tetradactylus* exhibits these same eight, deciduous loci in its lower jaw, but only four clearly differentiated tooth buds in the upper. Based on their positions relative to the lowers, these are likely dC, dP2, dP3, and dP4. Molars are absent in this specimen. When evident in our youngest prenatal specimens, the dp1 is among the smallest and least developed loci (Fig. 2). A small successional lamina is evident attached to the di1, dP3, and dP4 in *E. myurus* (UMZC 2016-histo-Ep2; Fig. 3), which are also the largest teeth in this specimen. No sign of a successional lamina is evident for dp1 in any of these specimens, consistent with the interpretation of Kindahl (1957) that macroscelidids lack a successional tooth for dp1.

Six histologically prepared specimens of *Procavia capensis* ranged in size from 26 mm to 80 mm CRL (Table 3). The smallest three (26, 28, 29 mm CRL) showed embryonic teeth corresponding to some but not all of their deciduous loci; the largest three (42, 60, 80 mm CRL) showed development at all of the antemolars and first molar present in postnatal specimens; the largest two (60, 80 mm CRL) also showed upper deciduous canines. The first premolar locus corresponds to the dp1 and is continuous with the primary dental lamina forming the other deciduous antemolars, as in macroscelidids.

PTA-stained, CT-scanned specimens of *Elephantulus myurus* in our sample with a CRL at or over 15 mm (Fig. 2; Table 2) also exhibit eight loci per quadrant. These do not appear linked to one another via an epithelial, con-

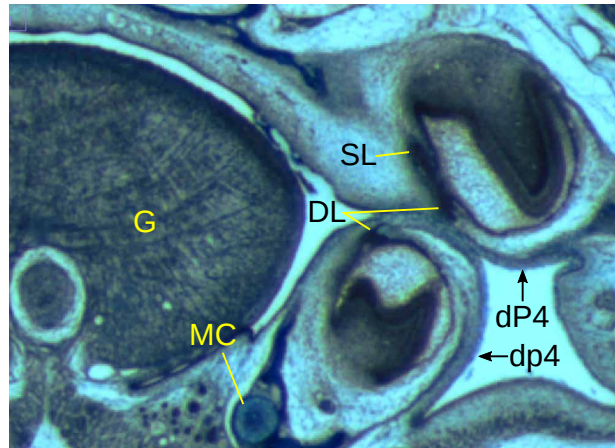


Figure 3. Coronal slice through UMZC 2016-histo-Ep2, *Elephantulus myurus* (slide 29, section 34) showing the oral cavity with developing tooth buds of dp4 and dP4. DL = dental lamina, G = genioglossus, MC = Meckel's cartilage, SL = successional lamina.

nective primary dental lamina, as seen histologically and in smaller specimens. However, based on spatial relationships and relative size, they are deciduous loci and include three incisors, one canine, and four premolars, of which dp1 is again the smallest (Fig. 2). Our second-smallest specimen (CRL 13.4 mm), shows an epithelial primary dental lamina from which tooth buds arise in both upper and lower jaws. In the upper jaws, tooth buds correspond to di1–3, dC, dP2–4; signs of a dP1 are lacking. Another specimen of similar size (CRL 14.2 mm) shows an incomplete set of early bell stage tooth buds arising from both upper and lower dental laminae. No tooth buds are evident in our smallest specimen (UMZC 2022.1.1, HL 5.4 mm). Successional laminae may be present, at least in the larger embryos, but are not obvious in any of our PTA-stained CT scans.

Except for one specimen showing a pair of supernumerary upper teeth (UMZC 2021.38 [w39]), our sample of near-term or postnatal *Macroscelides proboscideus* with known age data exhibited the same dental formula at varying degrees of eruption. The deciduous generation consisted of upper and lower di1–3, dc, and dp1–4, the permanent generation i1–3, c, an unreplaced dp1, p2–4, and m1–2. All postnatal specimens showed at least partly mineralized deciduous first premolars; none of the teeth at the first premolar locus exhibited any signs of replacement. Ages ranged from 0 to 1,982 days post-birth; 13 of the 16 were between 0–195 days (Table 1).

Asher and Olbricht (2009) referred to the upper and lower first premolar in macroscelidids as a “p1”, implying without further justification that this was a replacement tooth. They did not actually test first premolar homology, but the eruption sequence they outlined is supported here with the addition of more specimens of known age. Specimens from birth to three days (Fig. 4A, 4B) have incompletely erupted deciduous teeth; except for dp1 with only a partly mineralized apex, deciduous crowns are largely mineralized. Molars are not evident. By 16 days (Fig. 4C), deciduous teeth are at or near full eruption ex-

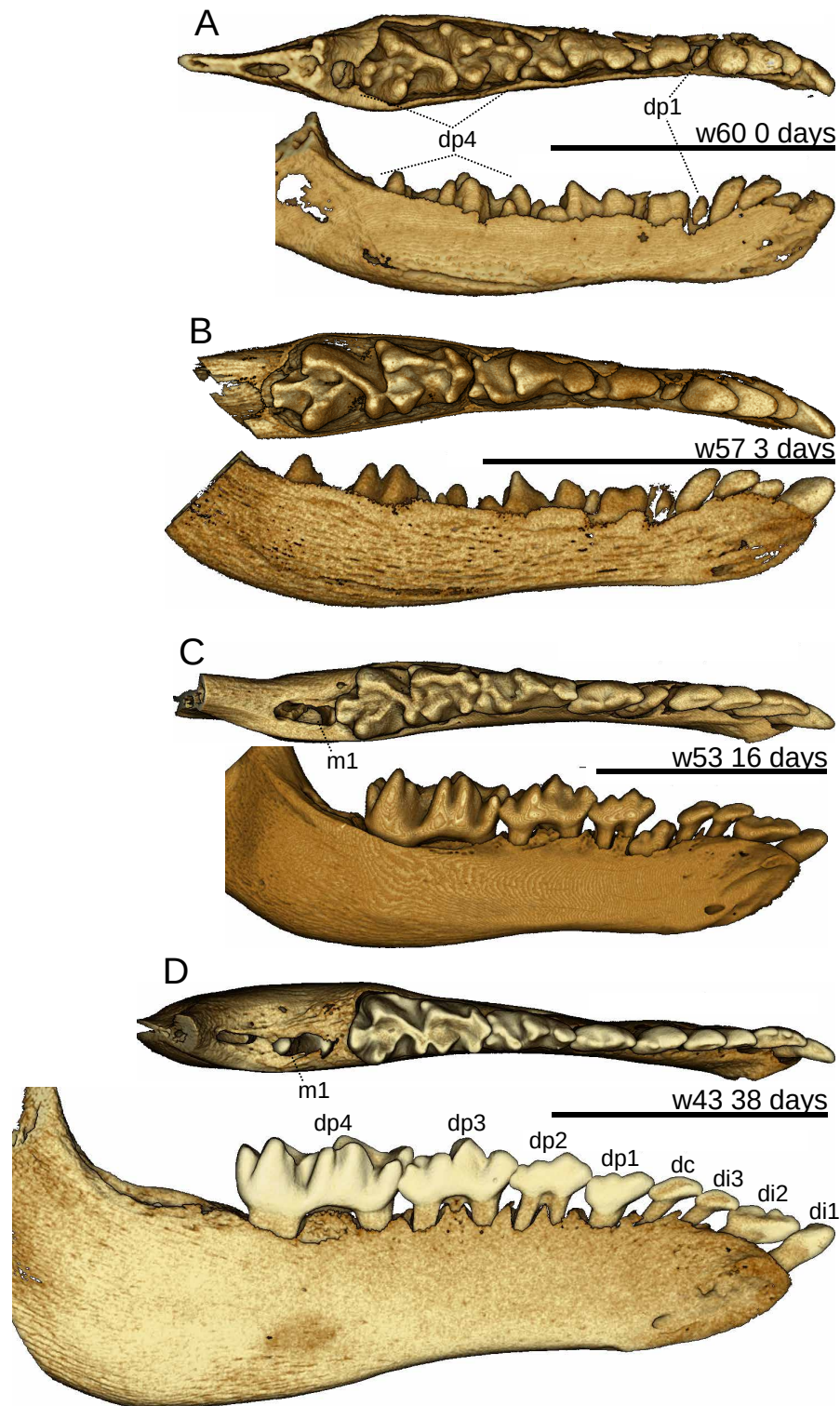


Figure 4. Occlusal (top) and lingual (bottom) views of *M. proboscideus* jaws of known age post-birth. All teeth are deciduous except as noted. Scale bars = 5mm. Scale bar in **D** applies to lingual view. Occlusal view is not to scale.

cept dp1. Among the permanent teeth, only m1 has begun to mineralize and there are no signs of any replacement teeth. By 38 days (Fig. 4D), dp1 has erupted, m1 is mineralized in its crypt; m2 and all replacement anteromolars except the apex of the canine crown remain unmineralized. By 69 days (Fig. 5A), di3 and dc have been shed with their permanent replacements partly (c) or fully (i3) erupted; p4 has approached full-mineralization followed by mineralized apices of p2 and p3; a high-crowned m1

has partly but not fully erupted and m2 has mineralized (Fig. 5A). By 101 days (Fig. 5B), di1–2 have been replaced and both molars have erupted; p2–4 are fully mineralized and have begun to pierce the alveolar plane. By 122 days (Fig. 5C), dp4 has been shed and dp2–3 nearly so. By 145 days, the complete permanent dentition (including a retained dp1) is fully erupted and functional. One specimen (UMZC 2021.38, field number w39, with a full adult dentition at 326 days of age) exhibited a bilat-

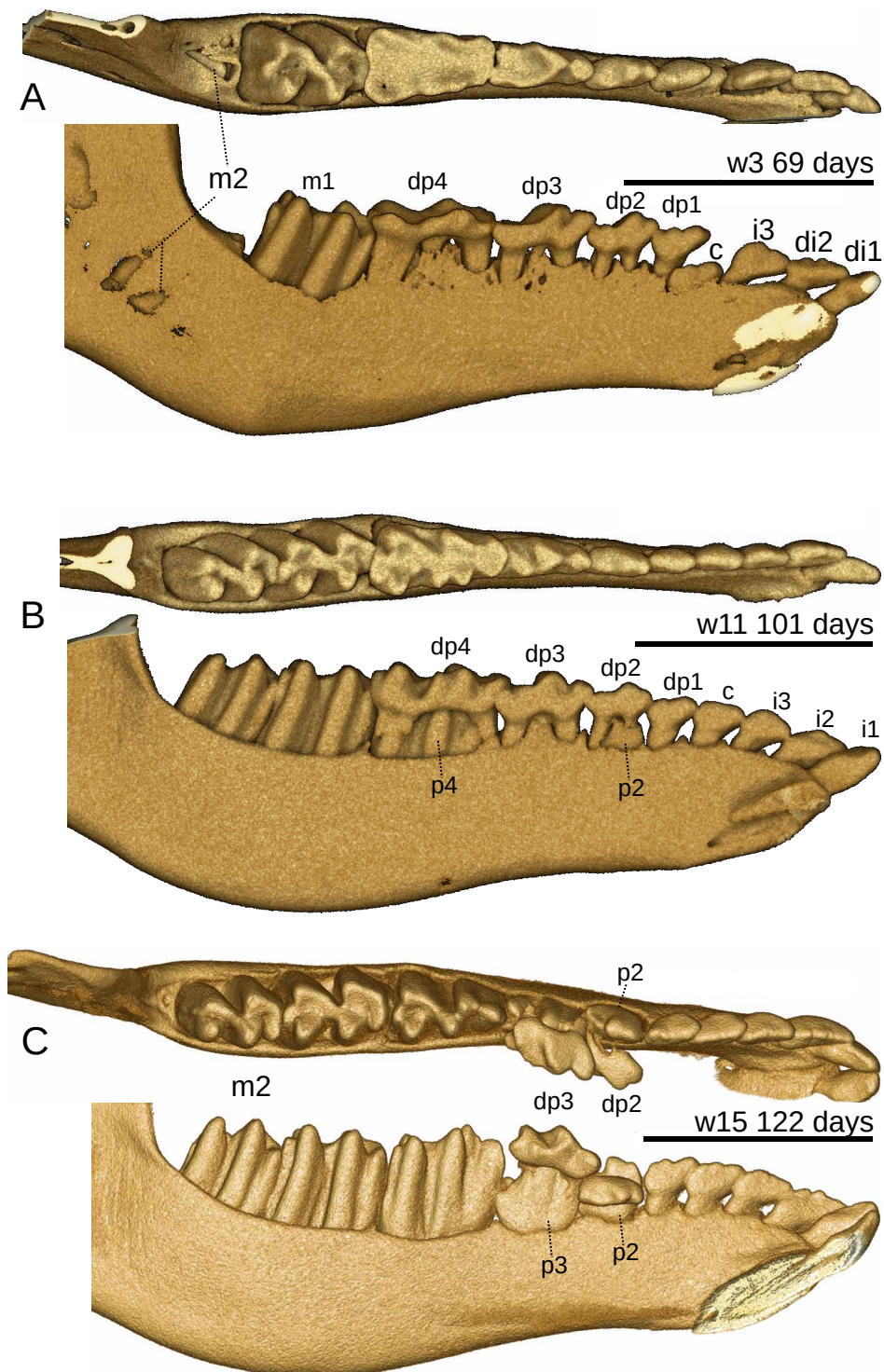


Figure 5. Occlusal (top) and lingual (bottom) views of *M. proboscideus* jaws of known age post-birth. Scale bars = 5mm.

eral, supernumerary, single-rooted tooth wedged between P3 and P4 in its maxilla.

Comparative developmental anatomy: canids

Our histologically prepared specimen of *Canis* (Table 3) showed seven tooth buds emanating from the primary dental lamina in each quadrant: dI1–3, dC, and dp2–4 (Fig. 6). The third and fourth premolar loci are the larg-

est, followed by the dC, dI3, dI2, dP2 and dI1. No sign exists of any emargination that might correspond with a deciduous first premolar, consistent with the results from Williams and Evans (1978).

CT scans of the youngest two specimens in our sample with known ages (*C. lupus familiaris* of the “pointer” breed) at 1 (Fig. 7A) and 5 (Fig. 7B) days post-birth lack any sign of a mineralized first premolar. By 5 days, two deciduous incisors, dc, dp2–4 and the apex of m1 are mineralized. The p1 locus remains unmineralized in a specimen 10 days of age (Fig. 7C). The apex of p1 shows

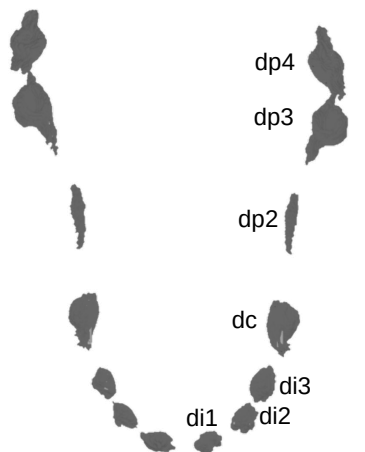


Figure 6. Reconstructed tooth buds of primary dental lamina of the lower jaw from *Canis* histological sections (UMZC 2016-histo-Cd1, 60mm CRL).

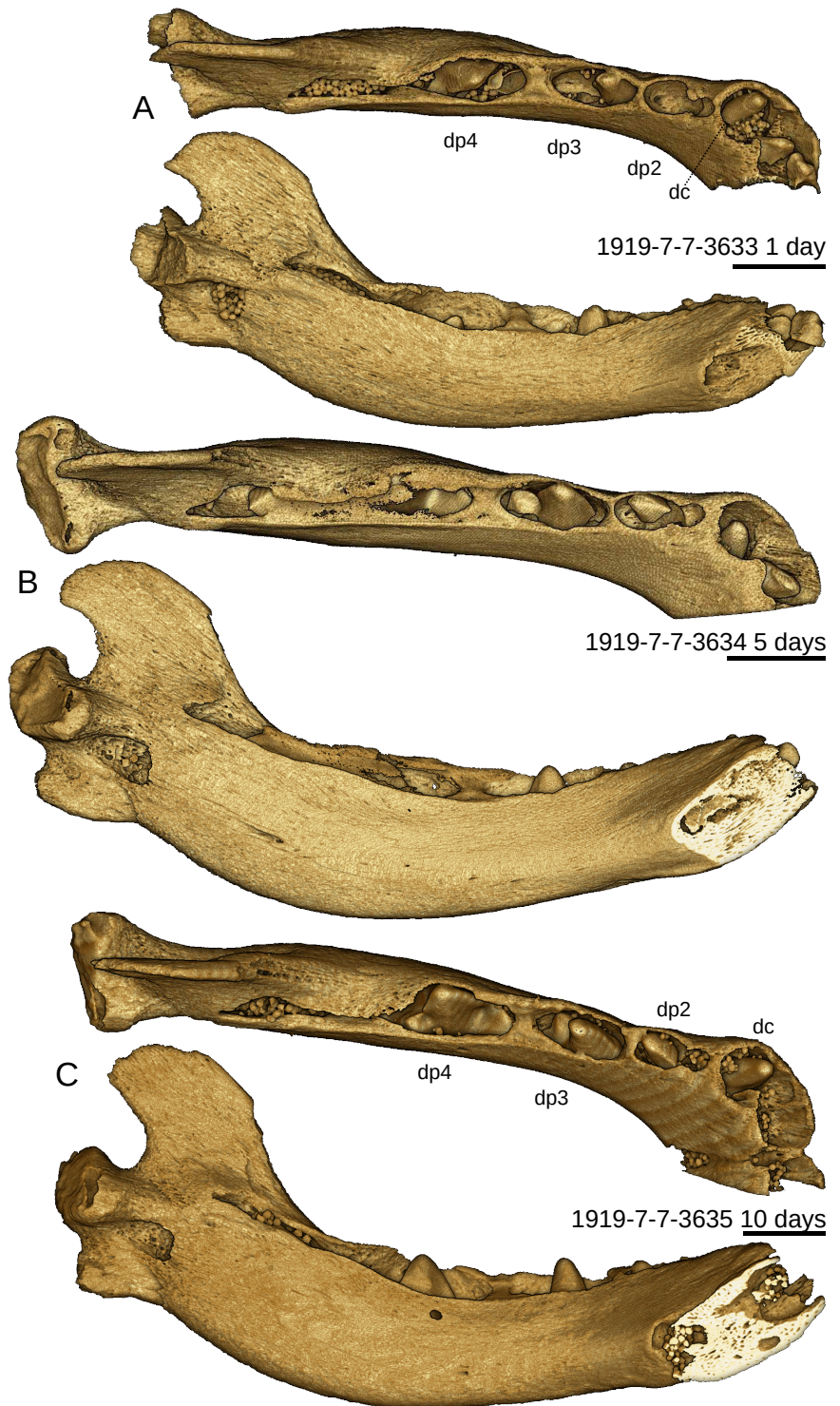


Figure 7. Occlusal (top) and lingual (bottom) views of *C. familiaris* (pointer) jaws of known age post-birth.

some mineralization in specimens of 18 (Fig. 8A) and 33 (Fig. 8B) days, specimens which have a symphysis-condyle length of 53 mm and 69 mm, respectively. The p1 crown is not fully mineralized in any of our specimens of known age (Figs. 7, 8); it is mineralized but still not fully erupted in another pointer specimen (Fig. 8C) with a longer symphysis-condyle length (115 mm) than our oldest age-documented pointer (69 mm, Fig. 8B). The mineralized but incompletely erupted p1 appears alongside an erupted deciduous dentition (Fig. 8C) as well as nearly all

permanent teeth still in their crypts: m1, a partly mineralized m2, p2, p3, p4, c and i1–3 (Fig. 9A). The smallest *Canis* in our sample with a fully erupted dentition, including p1, is a coyote (*C. latrans*, UMZC K3341) with a jaw length of 149 mm. Unlike *Macroselides* (Fig. 9B), first premolar mineralization and eruption in *Canis* corresponds more with the development of the replacement than deciduous teeth (Fig. 9A), supporting the inference of Williams and Evans (1978) that *Canis* lacks a functional, deciduous precursor at the p1 locus.

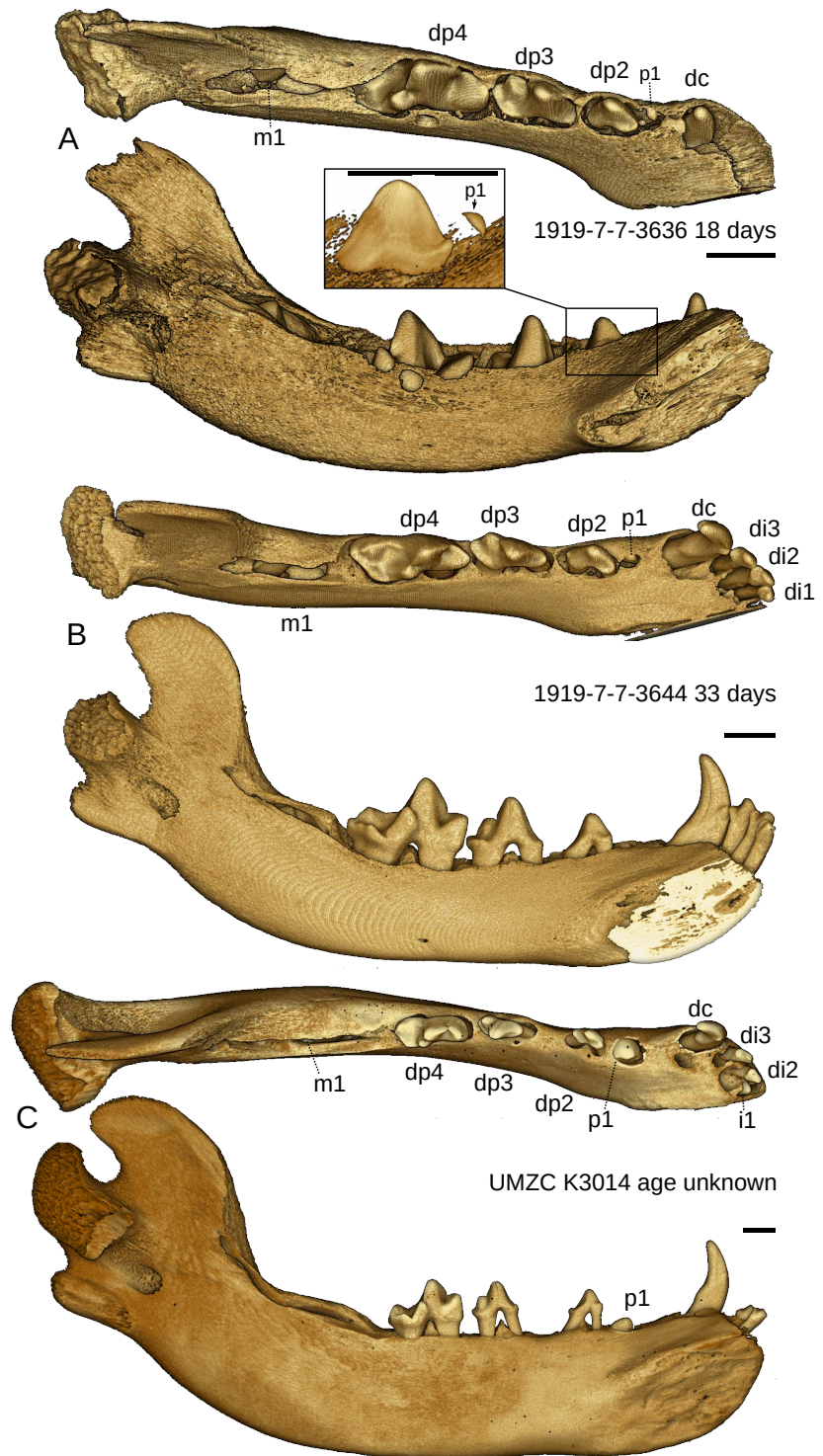


Figure 8. Occlusal (top) and lingual (bottom) views of *C. familiaris* jaws of known age post-birth (A, B) and another pointer (C) of unknown age but at a slightly later stage of dental development. Boxed Inset in A shows closeup of dp2 and mineralized apex of p1. Scale bars = 5mm.

Area predictions from the inhibitory cascade

Some fossil hyracoids simultaneously exhibit an erupting p1 below their dp1 (Gheerbrant et al. 2007; Asher et al. 2017), although we have yet to observe a *Procavia* specimen simultaneously exhibiting a dp1 with an erupting p1 below it. Nonetheless, both fossil and living hyracoids show clear anatomical differences in dp1 vs. p1 morphology (Fig. 10). It is therefore possible to contrast predicted vs. actual size for both p1 generations. In the fossil genera

in our sample (*Thyrohyrax* and *Sagatherium*), areas of dp2 and dp3 (in the form of 2B–C as discussed above) more accurately predict dp1 area than p1 area (Fig. 11); for one specimen of *T. litholagus* (DPC 20624), the prediction is very close (15.4 mm² observed, 15 mm² predicted). Predictions are less accurate for specimens of *Sagatherium*; these range from 1.8 to 4.8 mm² and show no overlap with observed dp1 areas (7.2 to 8.7 mm²). One predicted dp1 area of *T. meyeri* (5.9 mm²) falls slightly short of its observed (7.4 mm²). For other specimens of *T. meyeri* and *S. boweni* (our three *T. litholagus* specimens

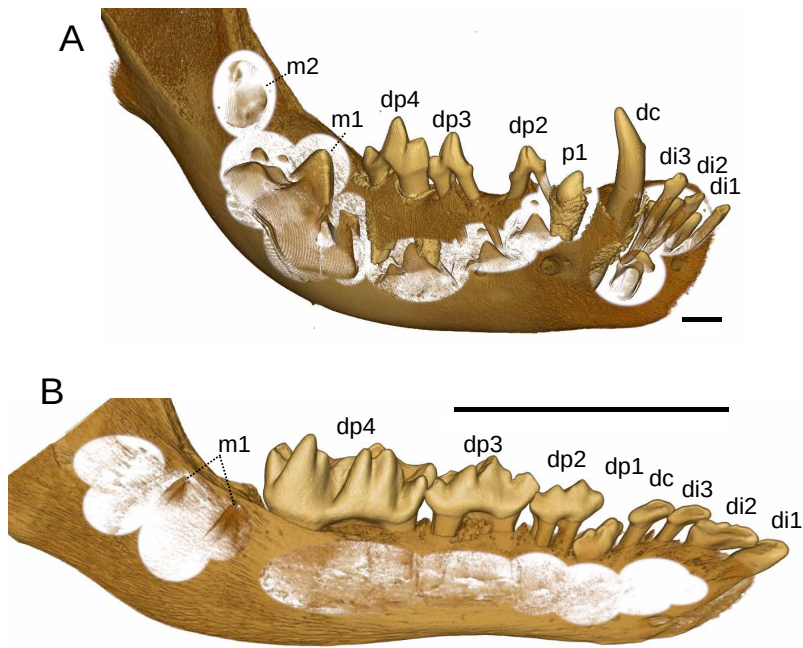


Figure 9. Virtually dissected jaws, both erupting the tooth at the first premolar locus, of **A)** *Canis lupus familiaris* (UMZC K3014, pointer) in antero-buccal view and **B)** *Macroscelides proboscideus* (UMZC 2011.1.4) in buccal view showing advanced mineralization of replacement teeth in *Canis* and lack thereof in *Macroscelides*. Scale bars = 5mm.

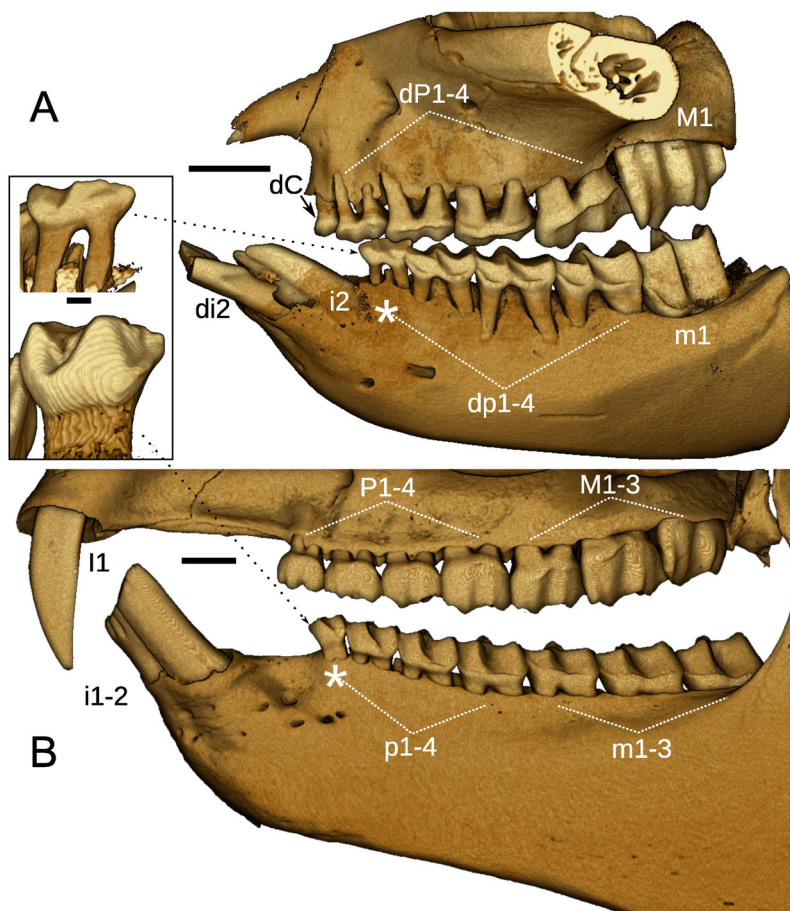


Figure 10. *Procavia capensis* specimens with **(A)**, UMZC H4981E) a deciduous dentition including upper and lower dp1 and upper dC and **(B)**, UMZC H5081A) a permanent dentition including replacement first premolar. Asterisks indicate p1 locus, shown also in lingual view by the inset with dotted arrows. Scalebar in inset = 1mm; scalebars in main figure = 5mm.

lack measurable p1 crowns), observed dp1 areas are 50%–100% smaller than p1 areas and closer to inhibitory cascade estimates (Fig. 11).

Extant *Procavia* variably exhibits a tooth at the first premolar locus. When present, the tooth may exhibit a narrow crown and two widely spaced roots typical of the deciduous generation, or it may have a more hypsodont crown

and a single or narrowly divided root, like a replacement anterior premolar (Fig. 10 and Asher et al. 2017: fig. 6). Hence, dp1 vs. p1 crowns of *Procavia* are anatomically distinguishable, but they overlap in terms of area, from 4.8–5.6 mm² (dp1) to 3.8–8.9 mm² (p1). Assuming crown and root anatomy reliably indicate first premolar homology, the inhibitory cascade does not better predict dp1 than

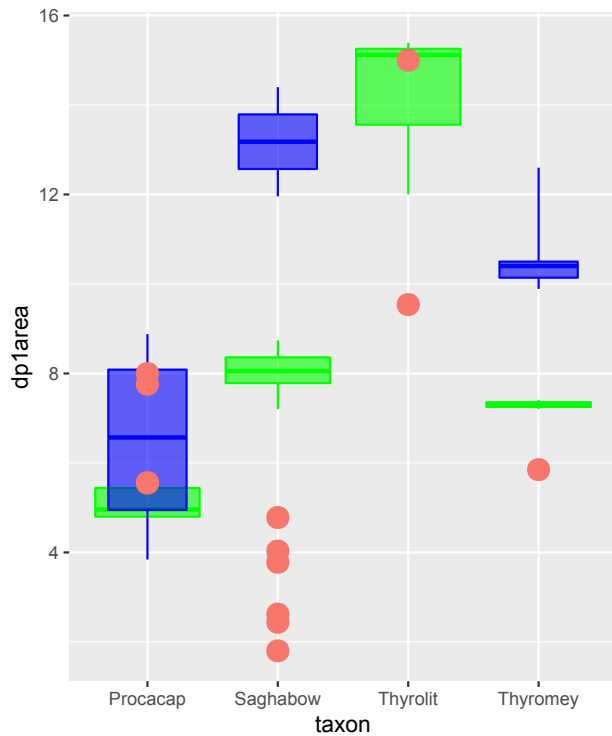


Figure 11. Predictions of dp1 area (y-axis) based on the inhibitory cascade (orange circles) in living and fossil hyracoids with distinct deciduous (green) and permanent (blue) generations at the first premolar locus. Procacap = *Procavia capensis*, Saghabow = *Sagatherium boweni*, Thyrolit = *Thyrohyrax litholagus*, Thyromey = *Thyrohyrax meyeri*.

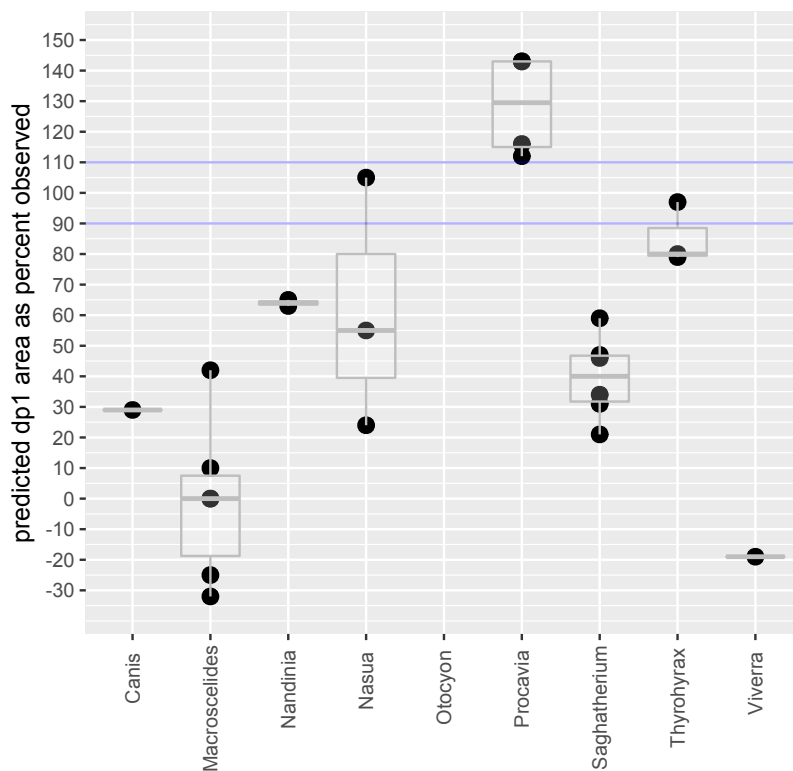


Figure 12. Predictions of dp1 area (y-axis) based on the inhibitory cascade, expressed as a percentage of the observed area of the first premolar (using dp1s in hyracoids). The area between the horizontal blue lines represents 90–110% of the observed first premolar area. Circles represent individual specimens, boxes middle quartiles, whiskers range.

p1 areas in *Procavia*. All predicted areas fall within the range of observed, permanent p1 areas; only two specimens approach the range evident in observed, deciduous p1 areas (UMZC 4981E, 4981C, both of which are predicted to have an area of 5.6mm²; see Fig. 11).

Supplementary Fig. S1 summarizes predicted vs. actual tooth areas for each genus. As a proportion of the observed first premolar area (and without distinguishing deciduous and replacement p1s in non-hyracoids), speci-

mens of two of the three hyracoid genera (*Thyrohyrax* and *Procavia*) and one carnivoran (*Nasua*) came closest to matching expectations of first premolar area based on the inhibitory cascade (Fig. 12). These taxa showed at least one specimen with a predicted area 86% or more of the observed. The fossil hyracoid *Sagatherium* and extant carnivoran *Nandinia* follow with at least one specimen with a predicted area comprising 59% of the observed. The genera in our sample with the least congruent predic-

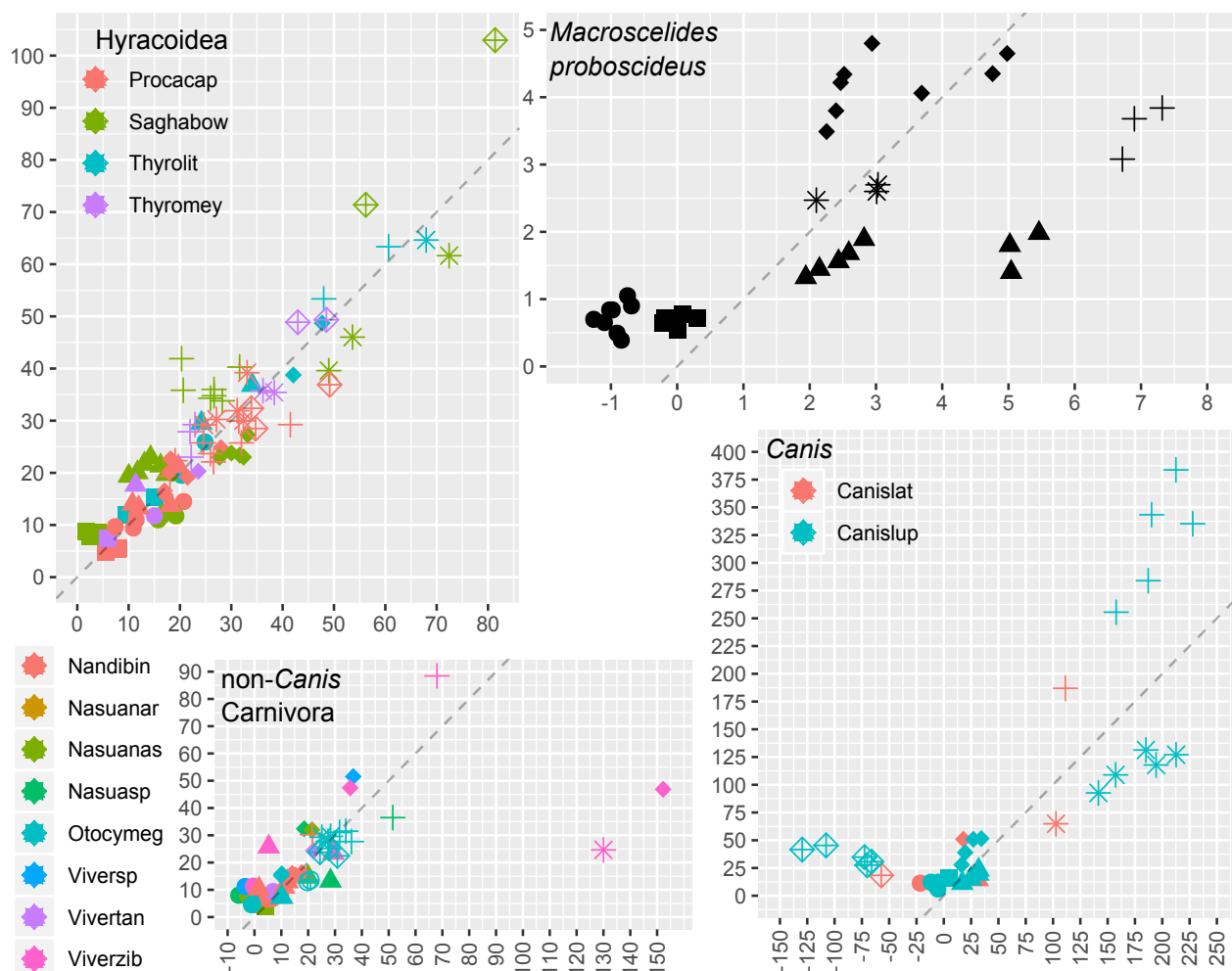


Figure 13. Predicted (x-axis) by actual (y-axis) areas of teeth in mm². Data for each genus are shown in Fig. S1. Dotted diagonal lines represent agreement between predicted and observed areas. first premolar=square, dp2=circle, dp3=triangle, dp4=diamond, m1=plus, m2=asterisk, m3=crossDiamond, m4=crossCircle. Canislat = *Canis latrans*, Canislup = *Canis lupus*, Nandibin = *Nandinia binotata*, Nasuanar = *Nasua narica*, Nasuanas = *Nasua nasua*, Nasuasp = *Nasua sp.*, Otocymeg = *Otocyon megalotis*, Procacap = *Procavia capensis*, Saghabow = *Saghattherium boweni*, Thyrolit = *Thyrohyrax litholagus*, Thyromey = *Thyrohyrax meyeri*, Viversp = *Viverra sp.*, Vivertan = *Viverra tangalanga*, Viverzib = *Viverra zibethica*.

tions of first premolar areas are *Canis*, *Macroscelides* and *Viverra*. One specimen of *Canis* (UMZC K3014) has a predicted first premolar area 29% of the observed. Three specimens of *Macroscelides* and one *Viverra* yield zero or negative area predictions using the inhibitory cascade (Fig. 12). According to area predictions from the inhibitory cascade, the first premolar of *Macroscelides* (as a dp1) should be closer to predicted values than the first premolar of *Canis* (as a p1). However, the area prediction expressed as a proportion of the observed in *Canis* falls within the range exhibited by *Macroscelides*. The closest prediction to an observed area in *Macroscelides* is specimen UMZC 2021-37 (field number w3) with 42%.

Across the deciduous and molar tooththrow, the taxa examined here vary in the extent to which predicted values approximate observed. The closest matches are hyracooids, and many individual area measurements fall on or close to the line indicating a 1:1 ratio of predicted to observed (Figs. 13, S1), particularly in the three specimens of the taxon with the largest body size, *Thyrohyrax litholagus*. The largest proportional deviations from this

line among hyracooids include a prediction of dp3 area that is half the observed (DPC 17844), and a prediction of dp2 area that is nearly twice the observed (DPC 16845). The closest predicted values in *Macroscelides* are for dp4 and m2, which deviate less than 10% of the observed (Fig. 13). Deviations at other loci are large, reaching as much as 3.6 times more than the observed for dp3 (Fig. 13) and showing zero or negative area estimates for dp1, as noted above (Fig. 12). Among non-*Canis* carnivorans, *Viverra* shows the largest deviations, with estimates for dp4 and m2 areas that are (respectively) more than three and five times greater than observed values. Predicted areas derived from one specimen of *Nandinia* (BMNH 26.7.6.162) are within 0.1mm² of its observed areas for dp2, dp3, and dp4. An *Otocyon* specimen (one of the only mammals that typically erupts four molars in each quadrant) shows similarly close predicted/observed values for m1, m2, and m3 (within 3% of observed), but has an m4 area roughly 50% smaller than expected. *Nasua* is the only carnivoran with at least one occurrence of a predicted dp1 area within 10% of the observed (Fig. 13).

Discussion and Conclusions

Homology determination based on origin of a given locus from the primary dental lamina has been considered sufficient evidence for identification as a deciduous locus. Indeed, as originally proposed (see Luckett 1993a), origin from the primary and not successional dental lamina is the definition of a deciduous tooth. Based on this criterion alone, the first premolar locus in *Canis* should be a dp1. Two lines of ontogenetic evidence arising from our dataset, also reflected in the conclusions of Kindahl (1957) and Williams and Evans (1978), lead us to regard this definition of deciduous teeth as insufficient: 1) the relatively early appearance of an embryonic first premolar toothbud in macroscelidids compared to *Canis* and 2) eruption of the functional tooth at the first premolar locus after mineralization of other functional teeth in *Canis* (Fig. 9A) and before in macroscelidids (Fig. 9B).

Van Nievelt and Smith (2005) identified permanent antemolars in the didelphid marsupial *Monodelphis* as successional, not deciduous. As in other marsupials, its only mineralized deciduous tooth is the last premolar or dp3, from which a successional lamina develops into the replacement p3. Like the tooth at the first premolar locus in *Canis*, other antemolars in *Monodelphis* appear to develop from the primary dental lamina without obvious successional laminae. Van Nievelt and Smith (2005: 338) wrote that “the apparent absence of even transitory, vestigial teeth in [*Monodelphis*] makes unambiguous identification of the generational homology of these permanent teeth difficult.” A lack of an obvious origin from a successional lamina in *Monodelphis* “would imply that the permanent teeth in [*Monodelphis*] are not homologous with those of [other] marsupials.” Yet marsupials such as *Dasyurus* (Luckett and Wooley 1996) and *Caluromys* (Van Nievelt and Smith 2005) show bud-stage rudiments in the primary dental lamina of at least some loci, from which successional laminae develop to eventually form the functional teeth. Hence, rather than identify permanent antemolars in *Monodelphis* as deciduous and *Dasyurus* as successional, Van Nievelt and Smith (2005:338) argued that “it is far more parsimonious ... to assume that in some marsupial taxa ... the vestigial first generation seen in other marsupials has been lost entirely. Therefore, the functional, permanent teeth observed in [*Monodelphis*] can most reasonably be interpreted as being homologous with the functional permanent teeth observed in other marsupials.” This implies that as-yet unobserved clusters of transient odontogenic cells in *Monodelphis* actually do appear during ontogeny, from which their replacements arose as a successional lamina. We agree with this interpretation.

The comparative anatomy and developmental timing of odontogenesis in macroscelidids and *Canis* supports the identification of their first premolars as, respectively, dp1 and p1. Our histologically prepared and CT-scanned specimens of macroscelidids, at the relevant developmental stages, consistently show a tooth developing from the primary dental lamina that corresponds to the dp1,

also evident in *Procavia*. As Kindahl (1957) noted, at no point do we observe a successional lamina arising from the macroscelidid first premolar locus. As Williams and Evans (1978) noted among *Canis* specimens, at no point do we observe a toothbud arising from the primary dental lamina that likely corresponds to a first deciduous premolar. Moreover, there is a substantial difference in the timing of post-birth mineralization in sengis compared to *Canis*, differences which correspond to the homology inferences made by Kindahl (1957) and Williams and Evans (1978). The first premolar in sengis mineralizes only slightly after the other deciduous teeth, and the mineralized apex of the dp1 crown is evident in CT scans of newborn specimens (Fig. 4A). No replacement teeth appear adjacent to their deciduous precursors during the first two weeks of development in *Macroscelides* (Figs 4, 9). At 16 days, *Macroscelides* with a nearly-erupted first premolar shows no sign of mineralized antemolars and just the apices of the m1 are evident in its crypt (Fig. 9B). Even at 38 days post-birth (Fig. 4D), when the dp1 is fully erupted, replacement antemolars are still not fully mineralized and at 69 days they are still not fully erupted (Fig. 5A).

Canis, in contrast, shows no sign of any mineralized tooth at the p1 locus until over two-weeks post-birth (Fig. 8A). At 18 days, the p1 and permanent canine have begun to mineralize. When it is finally mineralized and partly-erupted at 33 days, the first premolar is surrounded by mineralized crowns of most permanent teeth in a pointer specimen that is of uncertain age but likely more than 33 days post-birth (Figs. 8C, 9A). These patterns of mineralization and eruption support the conclusions of Kindahl (1957) that the first premolar in macroscelidids belongs to the deciduous generation and is never replaced, and of Williams and Evans (1978) that the first premolar in *Canis* is a successional tooth without a deciduous predecessor.

While the anatomical data are reasonably clear, there is nonetheless still a possibility that a key ontogenetic stage is missing that might overturn these conclusions about homology. The inhibitory cascade hypothesis has previously been discussed in terms of the posterior-most teeth of the primary dental lamina, the molars, and has been able to predict molar areas in a number of cases (Kavanagh et al. 2007; Evans et al. 2016). Our application of the IC model to more anterior loci is novel and based on the possibility that IC area estimates could help resolve the question of p1 homology. At least as quantified here, it does not. Neither *Macroscelides* nor *Canis* exhibited first premolar crown areas expected by the inhibitory cascade model; indeed, for some specimens of the former, predicted areas based on 2B-C (i.e., twice the area of dp2 minus dp3 to infer predicted area for dp1) yielded values at or below zero (Fig. 12).

With the linear representations of crown size used here, hyracoids deviate less from inhibitory cascade predictions across their tooththrow compared to macroscelidids and carnivores (Figs. 13, S1). The largest hyracoid in our sample, the fossil *Thyrohyrax litholagus*, exhibits particularly close matches of predicted to observed areas over most of its tooththrow (Fig. 13). This is not simply

due to reduced measurement error in larger vs. smaller specimens, as taxa with comparably-sized or larger teeth (e.g., some loci in *Sagatherium* and *Canis*) depart more from predicted areas than does *T. litholagus*. However, even in *Thyrohyrax*, most individuals have dp1s outside of the range predicted by the inhibitory cascade (Figs. 11, 12). Of course, areas calculated here using simple rectangles do not do justice to the diversity of crown size and shape, and improved methods for representing this diversity may yield different results. Until such methods are forthcoming, and at least for our sample, the inhibitory cascade hypothesis does not reliably distinguish first premolar homology based on predicted areas.

It is still worth noting that the four of the five taxa with the closest matches of observed to predicted first premolar area (*Thyrohyrax*, *Procavia*, *Nasua*, and *Sagatherium*; see Fig. 13) show, on average, steadily increasing areas from anterior to more posterior deciduous and molar cheek teeth. The two most widely divergent estimates (*Viverra* and *Macroselides*) correspond to taxa with a substantial change in the midst of the tooththrow, with $dp4 < m1 > m2$ in *Viverra* and $dp3 < dp4 > m1$ in *Macroselides* (as noted in hominins by Evans et al. 2016). The possibility that selection acting on such size differences in the midst of a tooththrow could override IC-predictions is worth further investigation.

In summary, and in contrast to our application of the IC model to infer generational homologies of mammalian teeth, anatomical data over the course of ontogeny support the first premolar homologies previously inferred for macroselidids and *Canis*. Our data are consistent with the conclusions of Kindahl (1957) that macroselidids retain a functional dp1 into adulthood which is never replaced. They also support the interpretation of Williams and Evans (1978) that canids erupt a successional tooth at the p1 locus which lacks a deciduous precursor.

Author contributions

RJA conceived of the project, collected and analyzed data, and wrote the paper. CJM contributed to project conception, collected and analyzed data, and helped to write the paper. CW, ES, HS, JL, SK, and NB contributed data, analysis and helped edit the text.

Acknowledgments

For help obtaining CT scans we thank Keturah Smithson at the Cambridge Biotomography Centre, Roberto Portelo Miguez and Vincent Fernandez at the NHM-London, Alan Heaver at the University of Cambridge Department of Engineering, Lionel Hautier at the University of Montpellier, Vera Weisbecker at Flinders University, Anjali Goswami at the NHM-London, and Madeleine Geiger and Marcelo Sánchez-Villagra at the University of Zürich. For access to CT scans on morpho-source.org, we acknowledge the United States National Museum, Yale Peabody Museum, the Field Museum of Natural History, Duke University Evolutionary Anthropology, Roger Benson, Doug Boyer, Jessie Maisano, April Neander, Tim Rowe, Blaire Van Valkenburgh, Greg Watkins-Colwell, and Angel Zeininger. For access to materials at the

Riksmuseet, Stockholm, we thank Olavi Grönwall, Bodil Kajrup, Daniela Kalthoff, and Per Erikson. We are grateful to Al Evans, Madeleine Geiger, Helder Gomes-Rodrigues, and Ingmar Werneburg for their constructive comments which have greatly improved our manuscript. In particular, Al Evans pointed out the implications of a size-shift along the tooththrow as a potential indication of adherence (or lack thereof) to inhibitory-cascade predictions. For financial support RJA thanks the Royal Society, the Leverhulme Trust, and the Department of Zoology, University of Cambridge. RJA and CJM thank the Synthesys programme of the European Union. The authors have no competing interests to declare that are relevant to the content of this article.

The authors are pleased to contribute to this volume in honor of Wolfgang Maier, emeritus Professor of Systematic Zoology at the University of Tübingen. RJA in particular wishes to acknowledge Herr Maier's generosity in serving as a mentor, not just during RJA's doctoral study in Tübingen during 1998-1999 but for his friendship and guidance over many subsequent years. Herr Maier greatly enhanced RJA's knowledge of systematics, vertebrate biology, histological anatomy, and overall career. I cannot express enough my gratitude to you, Prof. Maier, for your willingness to take me on as your student during that year in Tübingen and as your friend in the years thereafter.

References

- Asher RJ (2019) Recent additions to the fossil record of tenrecs and golden moles. *Afrotherian Conservation* 15: 4–13.
- Asher RJ, Gunnell GF, Seiffert ER, Pattinson D, Tabuce R, Hautier L, Sallam HM (2017) Dental eruption and growth in Hyracoidea (Mammalia, Afrotheria). *Journal of Vertebrate Paleontology* 37: e1317638. <https://doi.org/10.1080/02724634.2017.1317638>
- Asher RJ, Olbricht G (2009) Dental ontogeny in *Macroselides proboscideus* (Afrotheria) and *Erinaceus europaeus* (Lipotyphla). *Journal of Mammalian Evolution* 16: 99–115. <https://doi.org/10.1007/s10914-009-9105-2>
- Butler PM (1937) Studies of the Mammalian Dentition.—I. The Teeth of *Centetes ecaudatus* and its Allies. In: *Proceedings of the Zoological Society of London.*, 103–132. <https://doi.org/10.1111/j.1096-3642.1937.tb00825.x>
- Ciancio MR, Castro MC, Galliari FC, Carlini AA, Asher RJ (2012) Evolutionary Implications of Dental Eruption in *Dasyopus* (Xenarthra). *Journal of Mammalian Evolution* 19: 1–8. <https://doi.org/10.1007/s10914-011-9177-7>
- Domning DP, Hayek LAC (1984) Horizontal tooth replacement in the Amazonian manatee (*Trichechus inunguis*). *Mammalia* 48: 105–128. <https://doi.org/10.1515/mamm.1984.48.1.105>
- Evans AR, Daly ES, Catlett KK, Paul KS, King SJ, Skinner MM, Nesse HP, Hublin JJ, Townsend GC, Schwartz GT, Jernvall J (2016) A simple rule governs the evolution and development of hominin tooth size. *Nature* 530: 477–480. <https://doi.org/10.1038/nature16972>
- Geiger M, Marron S, West AR, Asher RJ (2020) Influences of Domestication and Island Evolution on Dental Growth in Sheep. *Journal of Mammalian Evolution* 27: 273–288. <https://doi.org/10.1007/s10914-018-9452-y>
- Gheerbrant E, Peigné S, Thomas H (2007) Première description du squelette d'un hyracoïde paléogène: *Sagatherium antiquum* de l'Oligocène inférieur de Jebel al Hasawnah, Libye. *Paleontographica Abteilung A* 279: 93–145.
- Gomes Rodrigues H, Marangoni P, Šumbera R, Tafforeau P, Wendelen W, Viriot L (2011) Continuous dental replacement in a hyper-chisel

- tooth digging rodent. Proceedings of the National Academy of Sciences 108: 17355–17359.
- Gomes Rodrigues H, Tabuce R, Asher RJ, Hautier L (2020) Developmental origins and homologies of the hyracoid dentition. *Evolution & development* 22: 323–335.
- Järvinen E, Tummers M, Thesleff I (2009) The role of the dental lamina in mammalian tooth replacement. *Journal of Experimental Zoology Part B: Molecular and Developmental Evolution* 312: 281–291. <https://doi.org/10.1002/jez.b.21275>
- Kavanagh KD, Evans AR, Jernvall J (2007) Predicting evolutionary patterns of mammalian teeth from development. *Nature* 449: 427–432. <https://doi.org/10.1038/nature06153>
- Kindahl ME (1967) Some Comparative Aspects of the Reduction of the Premolars in the Insectivora. *Journal of Dental Research* 46: 805–808. <https://doi.org/10.1177/00220345670460053401>
- Kindahl ME (1957) Some observations on the development of the tooth in *Elephantulus myurus jamesoni*. *Arkiv for Zoologi* 11: 21–29.
- Leche W (1907) Zur Entwicklungsgeschichte des Zahnsystems der Säugethiere: Die Familien der Centetidae, Solenodontidae und Chrysochloridae. *Zoologica, Stuttgart* 20: 1–157.
- Limaye A (2012) Drishti-volume exploration and presentation tool. In: *Proc Spie.*, 85060X–85060X.
- Lukkett WP (1993a) An Ontogenetic Assessment of Dental Homologies in Therian Mammals. In: Szalay FS, Novacek MJ, McKenna MC (Eds), *Mammal Phylogeny*. Springer, New York, 182–204. https://doi.org/10.1007/978-1-4615-7381-4_13
- Lukkett WP (1993b) Ontogenetic staging of the mammalian dentition, and its value for assessment of homology and heterochrony. *Journal of Mammalian Evolution* 1: 269–282. <https://doi.org/10.1007/BF01041667>
- Lukkett WP, Maier W (1982) Development of deciduous and permanent dentition in *Tarsius* and its phylogenetic significance. *Folia Primatologica* 37: 1–36. <https://doi.org/10.1159/000156018>
- Maier W (1984) Tooth Morphology and Dietary Specialization. In: Chivers DJ, Wood BA (Eds), *Food Acquisition and Processing in Primates*. Springer, Boston, 303–330. https://doi.org/10.1007/978-1-4757-5244-1_13
- O’Meara RN, Asher RJ (2016) The evolution of growth patterns in mammalian versus nonmammalian cynodonts. *Paleobiology* 42: 439–464. <https://doi.org/10.1017/pab.2015.51>
- Owen R (2011) *Odontography; or, A treatise on the comparative anatomy of the teeth; their physiological relations, mode of development, and microscopic structure, in the vertebrate animals*. Bailliere. <https://doi.org/10.5962/bhl.title.45634>
- Polly PD (2007) Evolutionary biology: Development with a bite. *Nature* 449: 413–415. <https://doi.org/10.1038/449413a>
- Popa EM, Anthwal N, Tucker AS (2016) Complex patterns of tooth replacement revealed in the fruit bat (*Eidolon helvum*). *Journal of Anatomy* 229: 847–856. <https://doi.org/10.1111/joa.12522>
- Roseman CC, Delezenne LK (2019) The Inhibitory Cascade Model is Not a Good Predictor of Molar Size Covariation. *Evolutionary Biology* 46: 229–238. <https://doi.org/10.1007/s11692-019-09480-y>
- Smith BH (2009) ‘Schultz’s Rule’ and the evolution of tooth emergence and replacement patterns in primates and ungulates. In: Teaford M, Smith M, Ferguson M (Eds), *Development, Function and Evolution of Teeth*. Cambridge University Press, Cambridge, 212–228. <https://doi.org/10.1017/cbo9780511542626.015>
- Tomes CS (1874) Memoirs: On the Existence of an Enamel Organ in an Armadillo (*Tatusia Peba*). *Journal of Cell Science* s2-14: 44–48. <https://doi.org/10.1242/jcs.s2-14.53.44>
- Tomes CS (1897) On the development of marsupial and other tubular enamels, with notes upon the development enamel in general. *Philosophical Transactions of the Royal Society of London. Series B, Containing Papers of a Biological Character* 189: 107–122. <https://doi.org/10.1098/rstb.1897.0012>
- Tucker AS, Fraser GJ (2014) Evolution and developmental diversity of tooth regeneration. In: *Seminars in Cell and Developmental Biology* 25-26:71–80. <https://doi.org/10.1016/j.semcdb.2013.12.013>
- Uhen MD (2000) Replacement of deciduous first premolars and dental eruption in archaeocete whales. *Journal of Mammalogy* 81: 123–133. [https://doi.org/10.1644/1545-1542\(2000\)081<0123:RODFPA>-2.0.CO;2](https://doi.org/10.1644/1545-1542(2000)081<0123:RODFPA>-2.0.CO;2)
- Ungar PS (2010) *Mammal teeth: origin, evolution, and diversity*. John Hopkins University Press, Baltimore.
- van Nievelt AFH, Smith KK (2005) To replace or not to replace: the significance of reduced functional tooth replacement in marsupial and placental mammals. *Paleobiology* 31: 324–346. [https://doi.org/10.1666/0094-8373\(2005\)031\[0324:trontr\]2.0.co;2](https://doi.org/10.1666/0094-8373(2005)031[0324:trontr]2.0.co;2)
- Williams RC, Evans HE (1978) Prenatal Dental Development in the Dog, *Canis familiaris*: Chronology of Tooth Germ Formation and Calcification of Deciduous Teeth. *Anatomia, Histologia, Embryologia* 7: 152–163. <https://doi.org/10.1111/j.1439-0264.1978.tb00665.x>
- Wilson LAB, Madden RH, Kay RF, Sánchez-Villagra MR (2012) Testing a developmental model in the fossil record: molar proportions in South American ungulates. *Paleobiology* 38: 308–321. <https://doi.org/10.1666/11001.1>
- Ziegler AC (1971) Dental homologies and possible relationships of recent Talpidae. *Journal of mammalogy* 52: 50–68. <https://doi.org/10.2307/1378431>

Supplementary material 1

Figure S1

Authors: McKay CJ, Welbourn-Green C, Seiffert ER, Sallam H, Li J, Kakarala SE, Bennett NC, Asher RJ (2022)

Data type: .pdf

Explanation note: Predicted (x-axis) by actual (y-axis) areas of teeth in mm² depicted for each species. Dotted diagonal lines represent agreement between predicted and observed areas. First premolar=square, dp2=circle, dp3=triangle, dp4=diamond, m1=plus, m2=asterisk, m3=crossDiamond, m4=crossCircle.

Copyright notice: This dataset is made available under the Open Database License (<http://opendatacommons.org/licenses/odbl/1.0>). The Open Database License (ODbL) is a license agreement intended to allow users to freely share, modify, and use this Dataset while maintaining this same freedom for others, provided that the original source and author(s) are credited.

Link: <https://doi.org/10.3897/vz.72.e78234.suppl1>

Supplementary material 2

Table S1

Authors: McKay CJ, Welbourn-Green C, Seiffert ER, Sallam H, Li J, Kakarala SE, Bennett NC, Asher RJ (2022)

Data type: .xlsx

Explanation note: CSV file listing specimens and measurements.

Copyright notice: This dataset is made available under the Open Database License (<http://opendatacommons.org/licenses/odbl/1.0>). The Open Database License (ODbL) is a license agreement intended to allow users to freely share, modify, and use this Dataset while maintaining this same freedom for others, provided that the original source and author(s) are credited.

Link: <https://doi.org/10.3897/vz.72.e78234.suppl2>